Polymer Sensors

DOI: 10.1002/ange.201404439

Fluorescence Sensing of Amine Vapors Using a Cationic Conjugated Polymer Combined with Various Anions**

*Sébastien Rochat and Timothy M. Swager**

Abstract: *A series of conjugated cationic polymers, differentiated only by their accompanying counter-anions, was prepared and characterized. The choice of counter-anion (CA) was found to drastically impact the solubility of the polymers and their optical properties in solution and in the solid state. Fluorescent polymer thin films were found to be instantaneously quenched by volatile amines in the gas phase at low ppm concentrations, and a mini-array with CAs as variable elements was found to be able to differentiate amines with good fidelity.*

Conjugated semiconducting polymers have found applications in organic electronics,[1] photovoltaics[1d,2] and (bio)-chemical sensing.[3] Efficient exciton migration in these materials provides sensitivity enhancements that have resulted in fluorescence-based sensing applications. Signal transduction is generally achieved by analyte-induced exciton quenching (fluorescence turn-off) or quenching sites removal (fluorescence turn-on), or by changes in the aggregation state of the polymer.[4,5] Many efforts in this area have focused on electron-donating polymers for the detection of electron-accepting analytes,[6] and the complementary use of electron-poor polymers for detection of electron-rich analytes has been limited to a few examples.[7] In addition to carefully adjusting the polymer's energy levels,[8] selectivity for a given analyte can be achieved by grafting specific receptors[9] or reactive moieties[10] onto conjugated polymer backbones. These approaches involve significant synthetic effort and require variations in monomers. Post-polymerization anion exchange is an efficient alternative strategy to modify conjugated polymers' optoelectronic properties,[11] charge transport,[12] hygroscopicity,[13] and electrostatic interactions with other electrolytes.[14] Herein we investigate the impact anion exchange has on the sensory responses, solubility, and optical properties (solution and thin films) of a cationic electron-poor conjugated polymer. We demonstrate that an array constituted with a fluorescent cationic conjugated polymer combined with four different counter-anions is able to detect and differentiate a series of industrially relevant amine vapors.

As starting material, we chose a conjugated cationic poly(pyridinium phenylene) (**PPymPh**) that was recently reported by our group, and that possesses pronounced photo-oxidizing properties as a result of its electron-accepting character.[15] When aqueous solutions of the original polymer **PPymPh:Cl** (**1**, chloride salt) are exposed to dodecyl sulfate (DS), perfluorinated tetraphenylborate (FTPB) or tetrafluoroborate (BF_4), the anion exchange reaction results in a very fast precipitation of compounds **PPymPh:DS** (**2**), **PPymPh:FTPB** (**3**), or **PPymPh:BF_4** (**4**) (Scheme 1), thereby allowing the isolation of pure compositions by consecutive washes and/or reprecipitation. The new electrolye pairs were characterized by NMR (^{1}H, and ^{19}F NMR when applicable), elemental analysis, and X-ray photoelectron spectroscopy (XPS). Although elemental analysis (C, H, N) data is of limited accuracy, XPS analysis confirms a very efficient anion exchange process, wherein the chloride ions are replaced by new anions (see the Supporting Information).

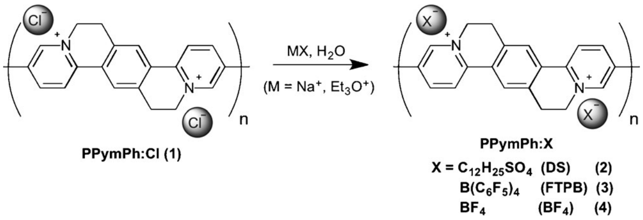

Scheme 1. Structure of **PPymPh:Cl** and anion metathesis reactions producing adducts **PPymPh:DS**, **PPymPh:FTPB**, and **PPymPh:BF_4**.

The solubility of the materials changes dramatically with counter-anion. In particular, **PPymPh:Cl** is only water-soluble, and displays no detectable solubility in common organic solvents (with the exception of trifluoroethanol, TFE). In contrast, **PPymPh:DS, PPymPh:FTPB**, and **PPymPh:BF_4** are not water-soluble, and display diverse degrees of solubility in organic solvents (see the solubility table (Table S1) in the Supporting Information). This tailored solubility by anion exchange is appealing for orthogonal solution deposition of multiple layers of polymers.

The optical properties of the polymers in different solvents are summarized in Table 1. The diverse solubilities complicate comparisons and there is no common solvent for all four polymers. Hence, we show in Figure 1a the absorbance of the four adducts in the solvents in which each of them displays the highest solubility. **PPymPh:Cl** (in H_2O) and **PPymPh:DS** (in TFE) display the expected absorbances with

---

[*] Dr. S. Rochat, Prof. Dr. T. M. Swager
Department of Chemistry and The Institute for Soldier Nanotechnologies, Massachusetts Institute of Technology
77 Massachusetts Avenue, Cambridge, MA 02139 (USA)
E-mail: tswager@mit.edu

[**] This research was supported by the Army Research Office through MIT's Institute for Soldier Nanotechnologies. S.R. acknowledges financial support from the Swiss National Science Foundation (Advanced Postdoctoral fellowship PA00P2-145389). We thank J. F. Fennell and Dr. J. Im for help with the XPS analyses.

Supporting information for this article is available on the WWW under http://dx.doi.org/10.1002/anie.201404439.

Table 1: Summary of optical properties of polymers **1**–**4** in selected solvents (**1**: H_2O; **2**: TFE; **3**: MeOH; **4**: DMF) and thin film formulations.

			1 (Cl)	**2 (DS)**	**3 (FTPB)**	**4 (BF_4)**
Solution[a]	Abs.	λ_{max} [nm]	412	409	418	(404)[b]
	PL	λ_{max} [nm]	426	423	433	–[c]
		Φ [%]	5.4	7.6	0.4	–[c]
		τ [ns]	0.2	0.3	0.5	–[c]
Film[d]	Abs.	λ_{max} [nm]	414	425	412	420
	PL	λ_{max} [nm]	547	541	553	542
		Φ [%]	57	21	11	40

[a] Same conditions as in Figure 1 a. [b] **PPymPh:BF_4** has a very broad, weak absorbance. [c] **PPymPh:BF_4** is non-emissive in DMF. [d] See the Supporting Information for details about thin film preparation.

a maximum at 412 and 409 nm, respectively. **PPymPh:FTPB** (in methanol) shows a slightly red-shifted absorbance maximum (418 nm) and a weak, broad absorbance band between 680 and 480 nm. **PPymPh:BF_4**, observed in DMF, shows a different spectrum, with the main absorbance band centred at 557 nm and a shoulder at 420 nm where the other polymers have their absorbance maxima. This behavior is indicative of an agglomeration-induced planarization and aggregation of the conjugated backbones in solution. Another insight is gained by observing the behavior of **PPymPh:FTPB** in different solvents. As shown in Figure 1 b, in acetonitrile or methanol, the main absorption band is located at 418 nm and a tailing absorbance is suggestive of some aggregation. In acetone this tailing absorption gains intensity at the expense of the primary absorption band, and in DMF the dominant absorbance is shifted to 569 nm. In addition to aggregation effects, this solvatochromism may be the result of Lewis basic interactions between the solvent molecules and the conjugated polymer backbone. As reported earlier,[15] this type of conjugated polymers are powerful electron acceptors, and the observation of these new intragap energy levels are very similar to the spectra of the reductively doped polymer.[15] Further, as shown in Figure S10 we find a correlation between the "donor number" of the respective solvent (representing its nucleophilic properties)[16] and the optical properties of polymer **PPymPh:FTPB**. Fluorescence measurements performed on polymers **1**–**4** in the same solvents as used for the absorbance measurements reflect the same trends (Figure 1 a): **PPymPh:Cl** (in H_2O) and **PPymPh:DS** (in TFE) display the expected sharp emission spectra with maxima at 426 and 423 nm, respectively. The associated quantum yields (Φ) were 5.4 and 7.6%. **PPymPh:FTPB** (in MeOH) is significantly less fluorescent ($\Phi = 0.4\%$), indicative of some degree of aggregation-induced quenching, and **PPymPh:BF_4** (in DMF) was found to be entirely non-emissive. Interestingly, **PPymPh:FTPB** was found to be significantly emissive only in MeOH, whereas solutions in acetonitrile, acetone and DMF were not emissive. Lifetime measurements indicate that **PPymPh:FTPB** in MeOH has a distinctly longer fluorescence lifetime ($\tau = 0.5$ ns) than either **PPymPh:Cl** ($\tau = 0.2$ ns in H_2O) or **PPymPh:DS** ($\tau = 0.3$ ns in TFE).

The optical properties of thin films made by spin-coating solutions of polymers **1**–**4** are depicted in Figure 1 c. Their absorbances are broadened relative to the solution spectra and the maxima are comprised between 412 and 425 nm, indicating a minimal influence of the counter-anion. The emission spectra are considerably red-shifted as compared to the solution spectra, and consist in broad, featureless peaks centred at 541–553 nm. Solid state quantum yields for thin films were estimated by comparing the integrations of the emission spectra with that of a known standard.[17] In order to minimize the influence of the thickness of the films, we employed films of relatively similar low optical densities.

Based on prior reports describing the response of fluorescent materials upon exposure to volatile reducing analytes,[18] and as a result of their high electron affinity,[7,19] we expected thin films of polymer adducts **1**–**4** to be well suited for the detection of vapors of volatile amines. The following experiments were carried out with a commercial FIDO sensor (FLIR Systems, Inc.) wherein polymer films are coated on the inner wall of a glass capillary and the fluorescence is continuously monitored.[20] This instrument was used to record the fluorescence response to analyte vapors generated at specific concentrations with a gas generator (Figure S11). The fluorescence quenching induced by amines is largely irreversible when the carrier gas is nitrogen, but in air a complete recovery of the initial emission intensity

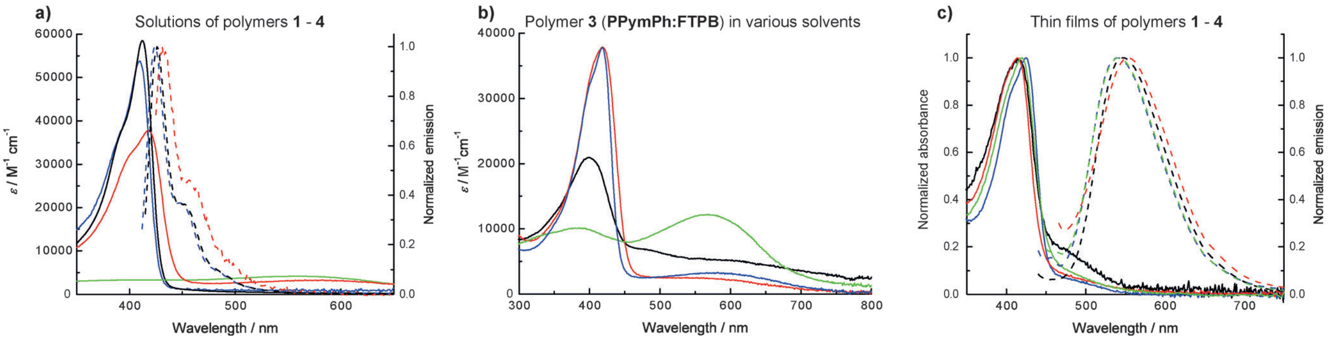

Figure 1. a) Absorbance (solid lines) and emission spectra (dashed lines) of polymers **1**–**4** (black, **PPymPh:Cl** in H_2O; blue, **PPymPh:DS** in TFE (trifluoroethanol); red, **PPymPh:FTPB** in MeOH; green: **PPymPh:BF_4** in DMF); b) Solvent-dependant absorbance of **PPymPh:FTPB** (blue, MeOH; red, acetonitrile; black, acetone; green, DMF) c) Absorbances (solid lines) and emissions (dashed lines) of thin films of polymers **1**–**4** (black, **PPymPh:Cl**; blue, **PPymPh:DS**; red, **PPymPh:FTPB**; green, **PPymPh:BF_4**).

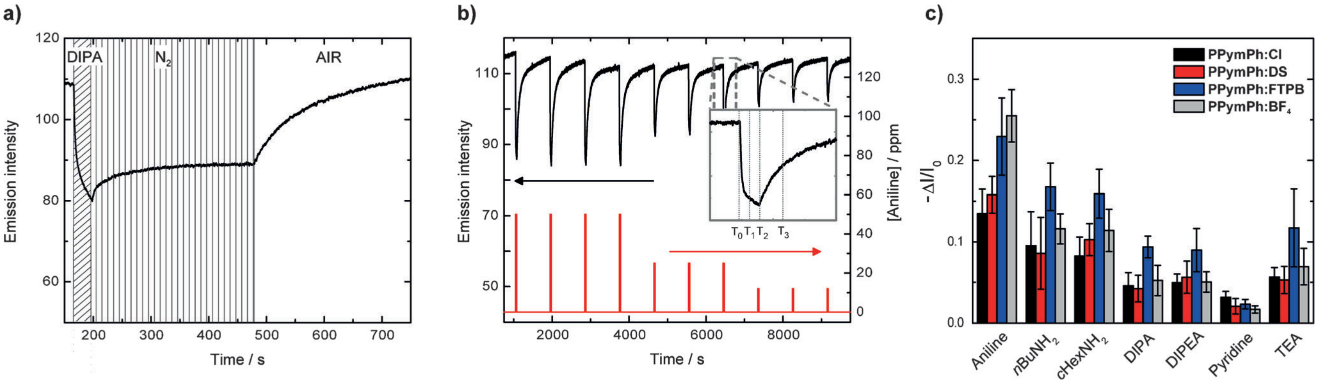

Figure 2. a) Time-resolved fluorescence intensity of a thin film of **PPymPh:DS** upon exposure to diisopropylamine (30 s) followed by pure nitrogen (270 s) and ambient air. b) Time-resolved fluorescence intensity (black trace) of a thin film of **PPymPh:BF$_4$** upon consecutive exposures to various concentrations of aniline vapors (30 s exposures, concentrations indicated by the red trace). Inset: Fluorescence change upon exposure to 25 ppm aniline, and definition of times T_0 (exposure starts), $T_1 = T_0 + 15$ s, $T_2 = T_0 + 30$ s (exposure stops), $T_3 = T_0 + 60$ s. c) Sensing response of a cross-reactive mini-array comprising the four polymer compositions. The quenching is measured after exposing each polymer to 100 ppm of the respective amine for 30 s (T_2).

is achieved (Figure 2a). This observation suggests that the photo-oxidative quenching of the amines is irreversible and reduced polymer is reset by air oxidation. Figure 2b shows consecutive exposures (30 s) of **PPymPh:BF$_4$** to various concentrations of aniline vapor. The response to concentration is linear and consecutive exposures indicate excellent reproducibility. The sensory polymers typically require 10–15 min exposure to an ambient air-flow to recover their initial fluorescence level. Considering the dose response and the background noise of the sensor, we determined a theoretical limit of detection for aniline (LoD) of 1.4 ppm (see Supporting Information and Figure S12 for details). More generally, the reproducibility limitations arise from device-to-device variability whereas the reproducibility of similar measurements on a single device is excellent.

We selected a series of industrially relevant amines (Table 2) and determined which polymer composition was most responsive to each amine. **PPymPh:FTPB** was found to be the most responsive to simple alkyl amines, whereas **PPymPh:Cl** is most responsive to pyridine and **PPymPh:BF$_4$** is better suited to detect aniline. As summarized in Table 2, detection limits in the low ppm range were achieved (except for pyridine with a LoD of 33 ppm), and hence these materials allow the detection of most analytes close to or below their safety limits (permissible exposure limit, PEL).[21] In particular, aniline, cyclohexylamine and triethylamine could be detected at concentrations below their respective PEL. An accurate determination of the LoD for diisopropylethylamine (DIPEA) was made difficult by the sensor's non-linear response. Although **PPymPh:FTPB** gave strong responses to DIPEA below 6 ppm, the non-linearity prevents the precise establishment of a lower practical LoD.

Table 2: Experimentally determined detection limits and safety recommendations for a series of industrially relevant volatile amines.

Analyte	Polymer	LoD [ppm]	PEL [ppm][21]
aniline	**PPymPh:BF$_4$**	1.4	5
n-butylamine	**PPymPh:FTPB**	6.3	5
cyclohexylamine	**PPymPh:FTPB**	5.6	10
diisopropylamine	**PPymPh:FTPB**	6.8	5
diisopropylethylamine	**PPymPh:FTPB**	6.0[a]	–
pyridine	**PPymPh:Cl**	33	5
triethylamine	**PPymPh:FTPB**	9.2	25

[a] For DIPEA, due to a lack of linear dosimetric response we report the lowest instrumentally accessible concentration that could be measured.

The differential responses of the four polymer compositions led us to explore their utility in a sensor array. Optical sensing of volatile analytes by sensor arrays was first pioneered by Suslick[22] and resulted in numerous practical innovations.[23] An array of the four materials was exposed to 100 ppm of seven selected amine vapors for 30 s, and the recorded emission quenching is given in Figure 2c. Amine-specific patterns are observed and the scattering in the data results from device-to-device variability from seven films of each material sequentially exposed to the seven amines in a semi-random order. No data pre-processing, correction or selection were performed, the only exception being the exclusion of the first exposure of each device to any amine, as these first exposures were sometimes not completely reversible. A more quantitative view of the performance of our sensor array is given by a linear discriminant analysis (LDA) performed on the data represented in Figure 2c. LDA is a statistical analysis method that seeks to classify analytes in predetermined classes (supervised method), thus allowing to quantify the performance of a sensing array.[24] When applied to the data represented in Figure 2c, LDA results in a modest 71% of analytes classified correctly (Table S2). In order to improve the discriminatory power of our mini-array, we included information related to the kinetics of the response. This approach has been shown to provide additional useful information for the discrimination of analytes.[8,25] When quenching intensities measured at T_1 (15 s exposure), T_2 (30 s exposure) and T_3 (30 s after exposure is stopped) are all used the discriminating power of our mini-array improved to correctly classifying 92% of the analytes (Figure 3). The limited degree of cross-selectivity is attributed to the use of four closely related sensory materials. More importantly, we

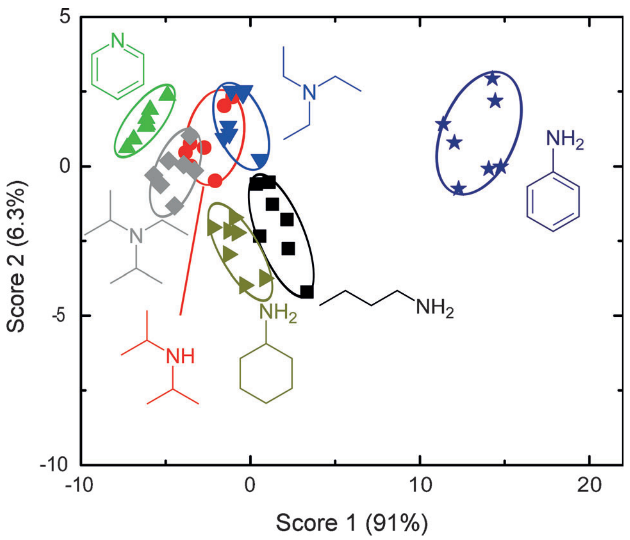

Figure 3. 2-Dimensional LDA score plot of a cross-reactive array made of polymers **1–4**.

performed cross-validation tests that indicate that an unknown analyte would be correctly identified in 88% of cases. Aniline, *n*-butylamine and pyridine are consistently correctly identified and occasional misidentifications mostly occur between DIPA, DIPEA and TEA, as would be expected by their clustering in Figure 3 (see also Tables S3 and S4). More precisely, when the unknown analyte is any of these three amines, there is a 76% probability the array returns the correct identity, and a 24% probability that the analyte is erroneously identified as one of the other two analytes. These limitations aside, it is remarkable that such a simple mini-array allows the differentiation of amine isomers (DIPA and TEA) and the closely related DIPEA with more than 75% success.

In conclusion, we demonstrated large changes in a cationic conjugated polymer's solubility, optical properties and sensory responses by anion exchange. This extremely convenient and simple method gives access to polymers with orthogonal solubility and with the ability to selectively detect volatile amines. Analyte-induced emission quenching allows amine detection at low ppm concentrations, below or close to their PEL values. Enhanced discrimination is achieved by exploiting time-resolved fluorescence measurements. This approach is in principle amenable to any reducing chemical species, and its scope can be enhanced or modulated by employing a greater diversity of counter-anions.

Received: April 17, 2014

Keywords: amine · amplification effect · conjugated polymer · fluorescence · sensors

---

[1] a) A. C. Grimsdale, K. L. Chan, R. E. Martin, P. G. Jokisz, A. B. Holmes, *Chem. Rev.* **2009**, *109*, 897–1091; b) C. Wang, H. Dong, W. Hu, Y. Liu, D. Zhu, *Chem. Rev.* **2012**, *112*, 2208–2267; c) X. Zhao, X. Zhan, *Chem. Soc. Rev.* **2011**, *40*, 3728–3743; d) P. M. Beaujuge, J. M. J. Fréchet, *J. Am. Chem. Soc.* **2011**, *133*, 20009–20029; e) L. Biniek, B. C. Schroeder, C. B. Nielsen, I. McCulloch, *J. Mater. Chem.* **2012**, *22*, 14803–14813.
[2] C. Li, M. Liu, N. G. Pschirer, M. Baumgarten, K. Müllen, *Chem. Rev.* **2010**, *110*, 6817–6855.
[3] a) C. Zhu, L. Liu, Q. Yang, F. Lv, S. Wang, *Chem. Rev.* **2012**, *112*, 4687–4735; b) P. Lin, F. Yan, *Adv. Mater.* **2012**, *24*, 34–51.
[4] a) S. Rochat, T. M. Swager, *ACS Appl. Mater. Interfaces* **2013**, *5*, 4488–4502; b) S. W. Thomas, G. D. Joly, T. M. Swager, *Chem. Rev.* **2007**, *107*, 1339–1386; c) T. M. Swager, *Acc. Chem. Res.* **1998**, *31*, 201–207.
[5] a) H.-A. Ho, A. Najari, M. Leclerc, *Acc. Chem. Res.* **2008**, *41*, 168–178; b) M. Leclerc, *Adv. Mater.* **1999**, *11*, 1491–1498; c) A. Duarte, K.-Y. Pu, B. Liu, G. C. Bazan, *Chem. Mater.* **2011**, *23*, 501–515; d) J. Liang, K. Li, B. Liu, *Chem. Sci.* **2013**, *4*, 1377–1394; e) C. V. Hoven, A. Garcia, G. C. Bazan, T.-Q. Nguyen, *Adv. Mater.* **2008**, *20*, 3793–3810; f) Y. Liu, K. Ogawa, K. S. Schanze, *J. Photochem. Photobiol. C* **2009**, *10*, 173–190; g) X. Duan, L. Liu, F. Feng, S. Wang, *Acc. Chem. Res.* **2010**, *43*, 260–270.
[6] a) J.-S. Yang, T. M. Swager, *J. Am. Chem. Soc.* **1998**, *120*, 11864–11873; b) L. Feng, H. Li, Y. Qu, C. Lü, *Chem. Commun.* **2012**, *48*, 4633–4635; c) L.-H. Zhang, T. Jiang, L.-B. Wu, J.-H. Wan, C.-H. Chen, Y.-B. Pei, H. Lu, Y. Deng, G.-F. Bian, H.-Y. Qiu, G.-Q. Lai, *Chem. Asian J.* **2012**, *7*, 1583–1593; d) G. He, N. Yan, J. Yang, H. Wang, L. Ding, S. Yin, Y. Fang, *Macromolecules* **2011**, *44*, 4759–4766; e) J. C. Sanchez, W. C. Trogler, *J. Mater. Chem.* **2008**, *18*, 3143–3156; f) L. Chen, D. W. McBranch, H.-L. Wang, R. Helgeson, F. Wudl, D. G. Whitten, *Proc. Natl. Acad. Sci. USA* **1999**, *96*, 12287–12292.
[7] a) S. Rochat, T. M. Swager, *J. Am. Chem. Soc.* **2013**, *135*, 17703–17706; b) Y. Kim, J. E. Whitten, T. M. Swager, *J. Am. Chem. Soc.* **2005**, *127*, 12122–12130.
[8] S. W. Thomas III, J. P. Amara, R. E. Bjork, T. M. Swager, *Chem. Commun.* **2005**, 4572–4574.
[9] a) A. I. Costa, H. D. Pinto, L. F. V. Ferreira, J. V. Prata, *Sens. Actuators B* **2012**, *161*, 702–713; b) L. Zhu, C. Yang, W. Zhang, J. Qin, *Polymer* **2008**, *49*, 217–224; c) B. Esser, T. M. Swager, *Angew. Chem. Int. Ed.* **2010**, *49*, 8872–8875; *Angew. Chem.* **2010**, *122*, 9056–9059.
[10] a) T.-H. Kim, T. M. Swager, *Angew. Chem. Int. Ed.* **2003**, *42*, 4803–4806; *Angew. Chem.* **2003**, *115*, 4951–4954; b) J. H. Wosnick, C. M. Mello, T. M. Swager, *J. Am. Chem. Soc.* **2005**, *127*, 3400–3405.
[11] a) R. Yang, A. Garcia, D. Korystov, A. Mikhailovsky, G. C. Bazan, T.-Q. Nguyen, *J. Am. Chem. Soc.* **2006**, *128*, 16532–16539; b) C.-S. Tsai, S.-H. Yang, B.-C. Liu, H.-C. Su, *Org. Electron.* **2013**, *14*, 488–499.
[12] A. Garcia, Y. Jin, J. Z. Brzezinski, T.-Q. Nguyen, *J. Phys. Chem. C* **2010**, *114*, 22309–22315.
[13] J. H. Ortony, R. Yang, J. Z. Brzezinski, L. Edman, T.-Q. Nguyen, G. C. Bazan, *Adv. Mater.* **2008**, *20*, 298–302.
[14] M. Kang, O. K. Nag, R. R. Nayak, S. Hwang, H. Suh, H. Y. Woo, *Macromolecules* **2009**, *42*, 2708–2714.
[15] D. Izuhara, T. M. Swager, *J. Am. Chem. Soc.* **2009**, *131*, 17724–17725.
[16] a) V. Gutmann, *Coord. Chem. Rev.* **1976**, *18*, 225–255; b) F. Arnaud-Neu, R. Delgado, S. Chaves, *Pure Appl. Chem.* **2003**, *75*, 71–102.
[17] J. A. Osaheni, S. A. Jenekhe, *J. Am. Chem. Soc.* **1995**, *117*, 7389–7398.
[18] a) P. Xue, Q. Xu, P. Gong, C. Qian, A. Ren, Y. Zhang, R. Lu, *Chem. Commun.* **2013**, *49*, 5838–5840; b) J. J. Peterson, A. R. Davis, M. Werre, E. B. Coughlin, K. R. Carter, *ACS Appl. Mater. Interfaces* **2011**, *3*, 1796–1799; c) Y. Che, X. Yang, Z. Zhang, J. Zuo, J. S. Moore, L. Zang, *Chem. Commun.* **2010**, *46*, 4127–

4129; d) Y. Che, X. Yang, S. Loser, L. Zang, *Nano Lett.* **2008**, *8*, 2219 – 2223.

[19] Y. Kim, T. M. Swager, *Macromolecules* **2006**, *39*, 5177 – 5179.

[20] C. J. Cumming, C. Aker, M. Fisher, M. Fox, M. J. La Grone, D. Reust, M. G. Rockley, T. M. Swager, E. Towers, V. Williams, *IEEE Trans. Geosci. Remote Sens.* **2001**, *39*, 1119 – 1128.

[21] http://www.osha.gov (retrieved 10/28/2013).

[22] N. A. Rakow, K. S. Suslick, *Nature* **2000**, *406*, 710 – 713.

[23] J. R. Askim, M. Mahmoudi, K. S. Suslick, *Chem. Soc. Rev.* **2013**, *42*, 8649 – 8682.

[24] P. C. Jurs, G. A. Bakken, H. E. McClelland, *Chem. Rev.* **2000**, *100*, 2649 – 2678.

[25] S. Rochat, J. Gao, X. Qian, F. Zaubitzer, K. Severin, *Chem. Eur. J.* **2010**, *16*, 104 – 113.